Optical Wireless Communications: System Model, Capacity and Coding

Jing Li (Tiffany)
Dept. of Electrical & Computer Engineering
Lehigh University
Bethlehem, PA 18015

Murat Uysal
Dept. of Electrical & Computer Engineering
University of Waterloo
Waterloo, Ontario N2L 3G1, Canada

Abstract— **This work is motivated by the need to understand the ultimate capacity of the outdoor long-distance optical wireless communication with intensity modulation and direct detection. The channel under weak atmospheric turbulence is modeled as a stationary ergodic channel with log-normal intensity fading, where signals experience asymmetric statistics due to on-off keying signaling. Ergodic channel capacity with several different values of channel parameter σ_z and outage probabilities are computed to provide an information-theoretic view of the channel. Turbo codes matched to the channel are also investigated to shed insight into how much can be achieved with the state-of-the-art coding schemes. It is shown that fixed rate turbo codes can perform close to the capacity when turbulence is weak, and that variable rate adaptive coding is necessary to bridge the gap when turbulence gets strong.**

I. INTRODUCTION

Optical wireless, also known as free-space optics, is a cost-effective and high bandwidth access technique and receives growing attention with recent commercialization success. Operating on unregulated spectrum, optical wireless has the potential of very high data rate, with potential applications ranging from deep-space/intersatellite communication and redundant links to search-and-rescue operations and solution for "last mile" problem.

This work considers outdoor long-distance optical wireless systems, where optical transceivers communicate directly along point-to-point line-of-sight propagation links. We first discuss the channel model under weak atmospheric turbulence, and then investigate the capacity of this channel. Depending on the nature of the application, different definitions of capacity are available in literature for fading channels. For non-real-time data services, ergodic capacity, which determines the maximum achievable information rate averaged over all fading states, is most commonly used. Other useful definitions include the delay-limited capacity for real-time data services and and outage capacity, for block fading (or quasi-static fading) channels. In this paper, we investigate the ergodic capacity of turbulence-dominant optical wireless links. We assume that ideal interleaving is performed over an infinitely long sequence and, hence, the channel is simplified to a memoryless, stationary and ergodic channel with independent and identically distributed (i.i.d.) intensity fading statistics. We consider cases where channel state information (CSI) is available at the transmitter only, at the receiver only, and at both.

What makes the problem interesting is that we consider intensity-modulation/direct-detection (IM/DD) with on-off keying (OOK), which is the only practical modulation that is deployed in commercial systems yet which is much less studied than the "typical" modulation schemes for wireless RF systems [3]. With OOK, the received signal demonstrates different statistics depending on whether "1" or "0" is transmitted, which makes the channel (or the output from the channel) appear asymmetric. Higher order modulation with heterodyne reception, although under active research, are still too complex and costly for practical systems. Hence, we expect our result to be useful for current and immediate future systems.

To evaluate the channel characteristics, we also examine the outage capacity of this channel. We compare it to that of RF Rayleigh fading channels to illustrate its relative "goodness". To give a feel of how much can be achieved with the state-of-the-art forward error control (FEC)q coding schemes, we evaluate turbo codes. The turbo decoder is modified to match to the channel characteristics. In addition to fixed rate codes, a variable rate adaptive turbo coding scheme is also presented and discussed. We show that variable rate codes are more efficient in bandwidth and power, and that it is indispensable to employ adaptive coding and/or power control in order to get close to the capacity throughput under (relatively) strong turbulence.

II. SYSTEM MODEL

A. Long-distance Optical Wireless Systems Using IM/DD

An outdoor long-distance optical wireless system consists of three parts: transmitter, propagation path and receiver. In order to accommodate the high-speed operation (e.g. 155 Mb/s or higher), the transmitter usually utilizes semiconductor lasers with broad bandwidth and high launch power. The receiver employs a transimpedance design, which makes a good compromise between bandwidth and noise, combined with bootstrapping that reduces the effective capacitance of the photodiode. Typical (bootstrapping) receivers use either (optically pre-amplified) PIN or avalanche photodiodes (APD) of different dimensions. IM/DD using OOK is widely deployed to modulate the signals. Fig. 1 illustrates a typical set-up of a long-distance point-to-point optical wireless system [4].

The power budget and raw-data performance of a LOS optical wireless link are subject to atmospheric loss along the propagation path, which includes free space loss, clear air absorption, scattering, refraction and atmospheric turbulence (or scintillation). Free space loss defines the proportion of optical power arriving at the receiver that is effectively captured within the receiver's aperture (see Fig. 1), and exists in all indoor and outdoor systems. Other forms of channel impairment are experienced only by outdoor systems. Air absorption, scattering and refraction are closely related to weather (e.g., fog, mist and snow). Nevertheless, field tests conducted in major cities around the world show that the atmospheric attenuation due to these factors is consistently low [5]. The dominant impairment to long-distance outdoor systems (500m to a few kilometers) is atmospheric turbulence, which occurs as a result of the variation in the refractive index due to inhomogeneities in temperature and pressure fluctuations. Atmospheric turbulence can be physically described by Kolmogorov theory [1], [2]. It causes the optical signal to scatter preferentially at very shallow angles in the direction of propagation, which, upon multiple signals (multiple laser strands), causes them to experience different phase shifts at they arrive simultane-

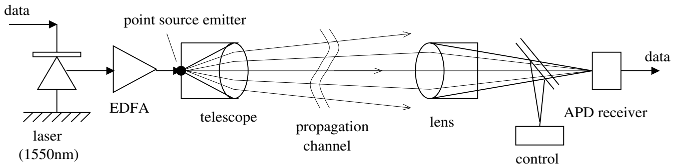

Fig. 1. A long-distance outdoor point-to-point optical wireless system. The propagation path schematically depicts free space loss.

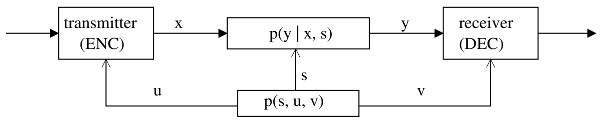

Fig. 2. Abstract system model for the optical wireless channel

ously at the receiver. This in turns results in random amplitude fluctuation of the detected signal.

B. Channel Model

Abstract Model – At the abstract level, we model an optical wireless channel as a discrete-time channel with stationary and ergodic time-varying intensity gain (i.e. channel state) S (≥ 0) and AWGN noise n. Fig. 2 plots the system model where X, Y, S, U and V denote transmitted signals, received signals, the channel state (i.e. intensity gain), CSI at transmitter and CSI at receiver, respectively. We consider binary input and continuous output, and assume that

$$f(y^n|x^n, s^n) = \prod_{i=1}^{n} f(y_i|x_i, s_i), \tag{1}$$

where $x_i \in \{0, 1\}$ and $y_i \in (-\infty, \infty)$.

Statistical Model – When the turbulence is relatively weak and the propagation distance is long, amplitude fluctuations may be modeled as a log-normal random variable [3]. The statistical channel model is thus characterized as:

$$y = sx + n = \eta I x + n \tag{2}$$

where $s = \eta I$ denotes the instantaneous intensity gain, $x \in \{0, 1\}$ the OOK modulated signal, $n \sim \mathcal{N}(0, N_0/2)$ the white Gaussian noise, η the effective photo-current conversion ratio of the receiver and I the turbulence-induced (normalized) light intensity. We have

$$\eta = \gamma \frac{e\lambda}{h_p c}, \qquad I = \exp(2Z), \tag{3}$$

where γ is the quantum efficiency of the photo receiver, e the electron charge, λ the signal wavelength, h_p Plank's constant, and c the speed of light. Z follows the Gaussian distribution with zero-mean and variance σ_z^2. Obviously, for a fixed optical wireless system, η is a constant and I follows log-normal distribution with mean $e^{2\sigma_z^2}$, variance $e^{4\sigma_z^2}(e^{4\sigma_z^2} - 1)$, and p.d.f.

$$f_I(z) = \frac{1}{2z\sigma_z\sqrt{2\pi}} \exp\left(-\frac{(\ln z)^2}{8\sigma_z^2}\right). \tag{4}$$

Detailed description of the physics underlying the optical wireless propagation channel can be found in [1], [2]. A good summary of the derivation of the log-normal amplitude fluctuation is presented in the pioneering work of [3]. We would like to point out that we use a somewhat different definition of the average signal-to-noise ratio (SNR) than [3]: instead of $\eta^2 \mathrm{E}[I]^2/N_0$ in [3], we define it to be

$$\bar{\gamma}_0 = \frac{\eta^2 \mathrm{E}[I^2]\, \mathrm{E}[X^2]}{N_0} = \frac{\eta^2 e^{8\sigma_z^2}}{2N_0}. \tag{5}$$

If BPSK instead of OOK is adopted, i.e., $x \in \{\pm 1\}$, the average SNR will be $\bar{\gamma}_1 = 2\bar{\gamma}_0$.

It is also worth noting that ambient light (i.e., stray light in addition to the wanted optical beam that reaches photodiode), although a major source of interference, is not considered in the above model. This is because the nature of the ambient light enables straight-forward remedies [4]. In practical systems, a narrowband infrared filter can be placed over the photodiode to filter out the majority of the ambient light originated from the out-of-band frequency. Furthermore, since ambient light is usually of low frequency (whose power spectrum density extends from DC to a few tens of kHz or, in rare cases, several hundreds of kHz), either a high-frequency subcarrier can be used to modulate the optical beam, or more popularly, a line code that contains no low-frequency components can be applied. Thus, the ambient light is essentially eliminated.

III. Capacity of log-normal Optical Wireless Channel with Side Information

A. CSI at Both Transmitter and Receiver

When perfect CSI is available at both transmitter and receiver, i.e., $S = U = V$, the mutual information is

$$I(Y;X|U,V) = I(Y;X|S) = \int_{-\infty}^{\infty} \sum_{x=0}^{1} \left[p(x|S) f(y|x,S) \log \frac{f(y|x,S)}{\sum_{m=0}^{1} p(m|S) f(y|m,S)} \right] dy \tag{6}$$

and the capacity is defined as $C \triangleq \max_{p(X|S)} I(Y;X|S)$. As mentioned before, the received signal takes different statistics on transmitting "On" and "Off" signals. This makes optimization difficult, since $I(Y;X|S)$ does not adopt a neat closed form. However, observe that

$$\begin{aligned} C &= \max_{p(X|S)} I(Y;X|S) = \max_{p(X|S)} \int_{-\infty}^{\infty} I(Y;X|s) f_s(s)\, ds \\ &= \int_{-\infty}^{\infty} \underbrace{\left(\max_{p(X|S)} I(Y;X|s) \right)}_{C_{\mathrm{AWGN}}(s,N_0)} f_s(s)\, ds, \end{aligned} \tag{7}$$

where $f_s(\cdot)$ is the p.d.f. of the channel state. The exchange of integration and maximization is possible because the channel we consider satisfies a compatibility constraint [7]. The compatibility constraint is said to be satisfied if (i) the channel sequence is i.i.d. and (ii) if the input distribution that maximizes mutual information is the same regardless of the channel state. Condition (i) follows from the assumption of i.i.d. input sequence and memoryless channel. For condition (ii), note that at each time instant, CSI is fixed and known, and the instantaneous OOK-signaled log-normal fading channel is an equivalent AWGN channel with binary input and continuous output. The optimal input distribution for this instantaneous channel is $P(0) = P(1) = 1/2$, which is independent of any particular channel state s. Hence, the ergodic capacity of this log-normal fading optical wireless channel with OOK and perfect CSI at both transmitter and receiver is given by

$$C(\bar{\gamma}_0) = \int_{-\infty}^{\infty} C_{\mathrm{AWGN}}(s, N_0) f_s(s)\, ds, \tag{8}$$

0-7803-7955-1/03/$17.00 (C) 2003 IEEE

TABLE I

CAPACITY OF OPTICAL WIRELESS CHANNEL WITH OOK

Es/No	Capacity (bit/symbol/Hz)		
(dB)	$\sigma_z = 0.1$	$\sigma_z = 0.2$	$\sigma_z = 0.3$
0	0.467565508	0.418368166	0.351412791
1	0.539768042	0.479538818	0.400396351
2	0.614261574	0.543019264	0.451838864
3	0.688280515	0.607180078	0.504923313
4	0.758671620	0.670193597	0.558703215
5	0.822292234	0.730190634	0.612150524
6	0.876517678	0.785444531	0.664215040
7	0.919733150	0.834552610	0.713889858
8	0.951643694	0.876580964	0.760275964
9	0.973265335	0.911143264	0.802638891
10	0.986574055	0.938397812	0.840451298
11	0.993939680	0.958965924	0.873417105
12	0.997567161	0.973792881	0.901475193
13	0.999140586	0.983984344	0.924784006
14	0.999735611	0.990652637	0.943691924
15	0.999929881	0.994799264	0.958699758
16	0.999984124	0.997246226	0.970417154

where $\bar{\gamma}_0$ is the average SNR given in (5), $f_s(s) = f_I(s/\eta)$ in (4), and $C_{\text{AWGN}}(s, N_0)$ is the capacity of the equivalent AWGN channel with binary input $\{0, s\}$ and Gaussian noise variance $N_0/2$, which, in turn, is equivalent to the capacity of the well-known BPSK AWGN channel evaluated at SNR of $\frac{s^2}{4N_0}$.

Tab. I lists the capacity in terms of average symbol SNR $E_s/N_0 = \bar{\gamma}_0$ as given in (8). Relatively weak turbulence with $\sigma_z = 0.1, 0.2$ and 0.3 is assumed. Fig. 3 plots the capacity curves along with that of a non-fading AWGN channel (OOK assumed for all cases), where the x-axis denotes the normalized bit SNR $E_b/N_0 = \bar{\gamma}_0/C$. Apparently, the AWGN case is the limit of the log-normal fading case for $\sigma_z \to 0$. We see that the channel capacity decreases considerably as atmospheric turbulence gets strong. It is also interesting to note that atmospheric turbulence incurs a bigger loss in E_b/N_0 at high rates than at low rates. This suggests that atmospheric turbulence can be a more detrimental factor for achieving high channel throughput than low throughput (assuming capacity-approaching coding is equally difficult for low and high rates alike).

B. CSI at Transmitter only

When CSI is only known to the transmitter, the capacity cannot exceed that of when CSI is available to both sides. It can be shown that it is no less either. This is because, according to Shannon's coding theorem [6], the case where $U = s$, and V and S are independent can be converted to an equivalent channel (in terms of capacity) with input W at the transmitter side, output Y at the receiver side. The observation $w = (x_1, x_2, \cdots, x_{|\mathcal{S}|})$ can be viewed as a function mapping the state alphabet to the input alphabet: $\mathcal{S} \to \mathcal{X}$ and there are $|\mathcal{X}|^{|\mathcal{S}|}$ such functions. The channel transition of the equivalent channel is given by

$$p(y|w) = p(y|x_1, x_2, \cdots, x_{|\mathcal{S}|}) = \sum_s p(s)p(y|x_s, s) \tag{9}$$

Shannon showed that for a finite alphabet of input, output and state sets $\mathcal{X}$, $\mathcal{Y}$ and $\mathcal{S}$, the capacity of the equivalent channel, and hence that of the original channel, is given by

$$C = \max_{q(w)} I(W; Y) \tag{10}$$

where $W \in \mathcal{X}^{|\mathcal{S}|}$ is a random vector of length $|\mathcal{S}|$ with elements in $\mathcal{X}$ and p.d.f. $q(w)$. In Shannon's original work, the theorem was proved for discrete memoryless channels. Using the techniques introduced by Gallager in [**?**], namely, partitioning and subdividing the state and the output space in finer scale, in the limit the same result will be obtained for the continuous state and continuous output case. The implication of the above coding theory is that, when perfect CSI is known to the transmitter, the channel capacity is achieved by the best resource allocation that is possible. Since the same optimal water-filling resource allocation can be performed prior to transmission (regardless of weather CSI is known to the receiver), there is no loss in channel capacity.

C. CSI at Receiver only

Despite the asymmetry introduced by the OOK modulation, the input distribution that maximizes the mutual information is uniform, which is invariant of the instantaneous channel state. As has been shown in [7], under compatibility condition, the capacity of the ergodic time-varying channel with CSI only at the receiver is the same as that with CSI at the transmitter also. An intuitive explanation is that, when s is known to the decoder, by scaling, the fading channel with instantaneous power gain s^2 is equivalent to a bandwidth-limited AWGN channel with noise power $\frac{N_0 B}{2s^2}$ per dimension (B is the bandwidth), and the whole fading channel is no more than a time-varying AWGN channel. Since the capacity achieving input distribution is independent of power adaptation and/or channel state, the same capacity as in (7) is achieved.

It should be noted that the above assumes that the input, channel states and Gaussian noise are i.i.d. In the case where the channel states are correlated, the capacity with CSI at the receiver only will be bounded from above by (7). To summarize, we have the following relations concerning the capacities of a generic stationary and ergodic, time-varying channel:

- Case 1: optimal input distribution varies with channel state

$$C_{\text{CSI at Tx and Rx}} \geq C_{\text{CSI at Tx}} > C_{\text{CSI at Rx}}$$

- Case 2: optimal input distribution is invariant and i.i.d. channel state

$$C_{\text{CSI at Tx and Rx}} = C_{\text{CSI at Tx}} = C_{\text{CSI at Rx}}$$

- Case 3: optimal input distribution is invariant and correlated channel state

$$C_{\text{CSI at Tx and Rx}} = C_{\text{CSI at Tx}} > C_{\text{CSI at Rx}}$$

IV. OUTAGE PROBABILITY

Another important statistical measure for the quality of a fading channel (especially slow fading) is the outage probability. Outage probability is generally defined as the percentage of time that the instantaneous quality of the channel is below a satisfactory threshold. Depending on how the channel quality is measured, it adopts different forms. For example, it can be conveniently defined as the probability of failing to reach a specified SNR value μ_{th} sufficient for satisfactory reception. This leads to the mathematical expression of

$$\xi \triangleq P\left(\frac{s^2}{N_0} < \mu_{th}\right) = P\left(\frac{\eta^2 I^2}{N_0} < \mu_{th}\right) = P\left(I < \frac{\sqrt{\mu_{th} N_0}}{\eta}\right).$$

From the p.d.f. of I in (4), we obtain the c.d.f.

$$F_I(x) = \int_{-\infty}^{x} f_I(z)dz = 1 - \frac{1}{2}\mathrm{erfc}\left(\frac{\ln x}{2\sqrt{2}\sigma_z}\right). \qquad (11)$$

Hence, the outage probability of this optical wireless channel is simply $F_I(x)$ evaluated at $x = \sqrt{\mu_{th} N_0}/\eta$. Applying the definition of average SNR $\bar{\gamma}_1 = \eta^2 e^{8\sigma_z^2}/N_0$ and denoting $\mu'_{th} \triangleq \mu_{th}/\bar{\gamma}_1$ as the normalized threshold, we have the outage probability:

$$\xi = 1 - \frac{1}{2}\mathrm{erfc}\left(\frac{1}{4\sqrt{2}\sigma_z}\ln(\mu'_{th}) + \sqrt{2}\sigma_z\right), \qquad (12)$$

Note that (12) does not consider the specific modulation in use, but instead assumes all signals have the same energy as in BPSK. Using the simple relation $\bar{\gamma}_1 = 2\bar{\gamma}_0$, we can evaluate the "equivalent" outage probability for OOK. Fig. 4 plots ξ versus μ'_{th} for several values of σ_z from 0.1 to 0.5. We see that the outage probability increases with σ_z. Note that the increase of σ_z has two counteracting impacts: (i) it improve the average light intensity $\mathrm{E}[I] = e^{2\sigma_z^2}$ (and thus the channel quality), and (ii) it also increases the variance of the fading and at a much faster rate: $\mathrm{Var}(I) = e^{4\sigma_z^2}(e^{4\sigma_z^2} - 1) \approx (\mathrm{E}[I])^4$. Severe variation in the light intensity increases the chance of outage and hence degrades the channel (Fig. 4). For comparison, the outage rate of Rayleigh fading channels as given by $\eta = 1 - e^{\mu'_{th}}$ is also shown. Although not an accurate comparison, we can roughly say that when $\sigma_z \leq 0.25$, the turbulence-dominant optical wireless channel is better than RF Raleigh channels, but as σ_z further increases, the channel quality deteriorates rapidly.

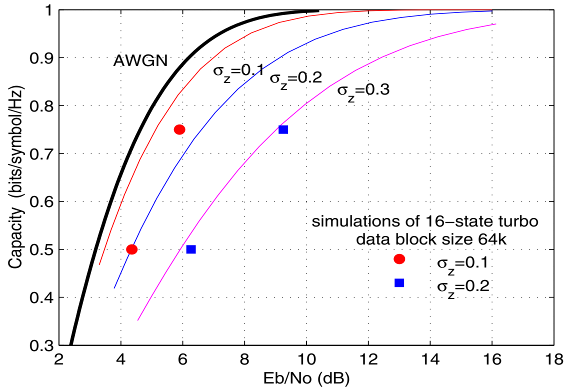

Fig. 3. Capacity of the log-normal fading optical wireless channel using OOK

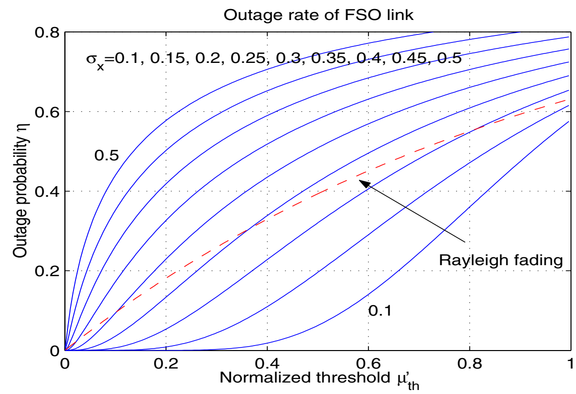

Fig. 4. Outage rate of optical wireless channels

V. Turbo Coding With Side Information

To shed light upon how much can be achieved with the state-of-the-art coding schemes, we evaluate the performance of turbo codes. We consider two specifications with generating polynomial (of the component code) given by $[1, (1 + D^2 + D^3 + D^4)/(1 + D + D^4)]$ and $[1, (1 + D^2)/(1 + D + D^2)]$, respectively. The former is one of the best 16-state turbo codes and has been shown to perform remarkably on a variety of channels including the RF Rayleigh and the long-haul fiber-optic channels. The later is a 4-state turbo code that is (relatively) simple yet still well-performing. We assume independent fading with perfect CSI known to the receiver. The original turbo code has rate $1/3$ and alternating uniform puncturing on parity bits is used to obtain higher rates.

The turbo decoder uses an iterative soft-in soft-out decoding strategy where maximum *a posteriori* probability (APP) decoding (i.e. the BCJR algorithm) is implemented for sub-decoders. For optimal performance, the BCJR algorithm needs to be adjusted to match with the channel characteristics. Specifically, the branch (transition) metric γ [8] needs to account for the channel response. Assuming log-domain implementation of the BCJR algorithm, the transition metric associated with the branch from state m' to m at time instant t for the aforementioned optical wireless channel is given by

$$\begin{aligned} &\gamma_t(m', m) \triangleq \log P(S_t = m, Y_t | S_{t-1} = m'), \\ &= \log P(a_t | S_t = m, S_{t-1} = m') + \log P(a_t) + \log P(Y_t | X_t), \\ &= \log P(a_t | S_t = m, S_{t-1} = m') + \log P(a_t) \\ &\quad + \Big(\frac{2\eta I_t}{N_0} < Y_t, X_t > + D\Big), \end{aligned} \qquad (13)$$

where a_t, X_t, Y_t and S_t denote the input to the encoder (user data), the output at the encoder (coded/modulated bits), received bits from the channel and the trellis state, all at time instant t, $P(a_t)$ denotes the *a priori* information of the user bit, and D is a constant that has no real impact on the soft output. With OOK signaling, X_t and Y_t are sequences of $\{0, 1\}$ bits (rather than ± 1 as in the binary phase shift keying case), and $< \cdot, \cdot >$ stands for inner product operation. For detailed discussion on the general BCJR algorithm, please refer to [8]; for detailed discussion on the application of the BCJR algorithm or the turbo decoding on optical wireless channels, please refer to [9].

The performance of turbo codes with decoder matched to optical wireless channels is plotted in Fig. 5. Extensive simulation is conducted to benchmark the performance of turbo codes with different rates, lengths, complexities and under different turbulence strengths. Each curve is marked with 4 parameters indicating the number of states (of the component code), the data block size, the code rate, and σ_z of the atmospheric turbulence, respectively. To see how close we are from the capacity limit, we also plot the simulation results of long turbo codes in Fig. 3. The performance is evaluated at BER of 10^{-5} with 6 decoding iterations. Under weak atmospheric turbulence ($\sigma_z = 0.1$), we see that 16-state turbo codes with large block sizes can perform within 1 dB from the capacity. However, as turbulence strength increases, the same code performs farther away from the capacity. This should not be surprising, since under severe intensity fluctuation, a much larger block size (i.e. a stronger code and a longer time averaging) is generally needed to achieve the same level of performance. The plot also implies that under strong turbulence, fixed-rate FEC codes alone are not sufficient to achieve near-capacity performance, and that adaptive coding and/or optimal power control are necessary in order to close the gap. For this reason we also investigate variable-rate adaptive coding in the sequel.

The basic assumption is that an error-free, zero-delay feedback channel is available, and that the measurement report in the feedback message includes bit error rate and/or signal variance (or pilot strength measurement), similar to what is specified in the rate adaptation for packet data services in 2nd and 3rd generation cellular standards like GPRS, CDMA IS-95 Rev B and CDMA2000. Hence, the transmitter can adapt to the changing channel conditions to maximize transmission power and bandwidth efficiency, sending more information with less error protection to achieve higher throughput when channel conditions are good, but using more powerful codes to ensure transmission reliability when channel conditions become worse.

Due to space limitation, a detailed discussion on the design criteria and approach as well as the rate adaptive rules of the variable rate turbo codes is omitted and can be found in [9]. Here we pinpoint the key points and present the results.

For efficient rate adaptivity and strong error correction capability, we construct variable rate turbo codes based on (punctured) 16-state turbo codes with the same generating polynomial as mentioned before. Instead of block interleavers and random interleavers, algebraic interleavers [10] [11] which can be generated pseudo-randomly on the fly without having to store the interleaving pattern are used. The family of codes we constructed possess the following three properties:

- *Rate compatibility* so that only a single encoder and decoder pair is required to deploy a class of variable rate FEC codes;
- *Constant bandwidth* to ensure smooth transmission and stable buffer utilization as the payload throughput changes; and
- *Large minimum distance* for good performance even with high rate codes.

As an example, Fig. 6 plots the simulation results of the set of variable rate turbo codes constructed using puncturing and algebraic interleaving whose code lengths are fixed to be 8K and code rates are $1/3$, $1/2$, $2/3$, $3/5$ and $3/4$. We see that each code is itself a powerful FEC code, and they collectively can achieve incremental performance improvement, thus permitting effective rate adaptation for low error probability over a large dynamic range of (instantaneous) SNRs. Although not shown (due to the space limitation), the performance of variable-rate adaptive turbo coding is evaluated for channel parameter $\sigma_z = 0.2$. Using a simple rate adaptation rule as described in [9], we see that adaptive coding can bridge the gap between fixed rate turbo coding and the ultimate channel capacity. In particular, we observe that whereas relatively strong atmospheric turbulence of $\sigma_z = 0.2$ has caused a single fixed-rate long turbo code (64K) to perform beyond 2 dB from the capacity (Fig. 3), a much shorter variable rate turbo code (8K) can close the gap by an additional 0.8 dB, which is quite encouraging. The rate adaptive coding scheme in use has a flavor of frame-by-frame power adaptation. In order to get further close to the capacity limit, we expect that (optimal) symbol-by-symbol power allocation is needed.

VI. Conclusion

We consider an outdoor long-distance optical wireless channel using IM/DD. Ergodic channel capacity with on-off keying and outage probability are computed, to provide insight into the quality of this channel as well as the ultimate performance limit. State-of-the-art turbo codes are also investigated to demonstrate how much has been achieved. We expect the results to be useful for current and immediate future systems.

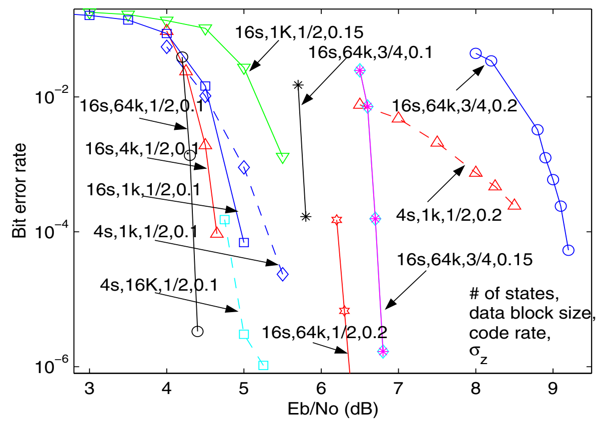

Fig. 5. Turbo codes on optical wireless channels

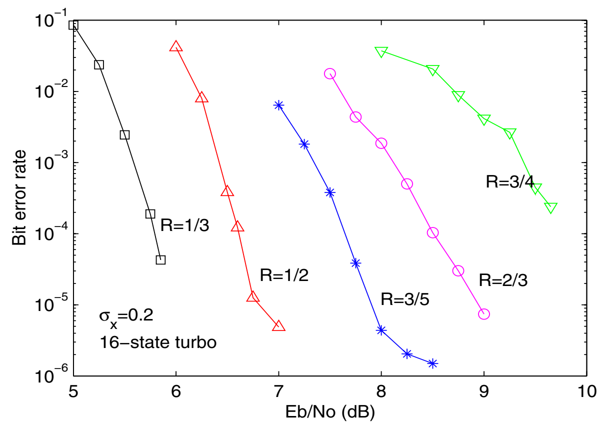

Fig. 6. A family of variable rate turbo codes with codeword length 8K

Acknowledgment

The authors wish to thank Wenyan He for his help in the preparation of the manuscript.

References

[1] A. Ishimaru, *Wave Propagation and Scattering in Random Media*, Academic, NY, 1978, vol. 1-2.

[2] S. Karp, R. Gagliardi, S. E. Moran, and L. B. Stotts, *Optical Channels*, Plenum, NY, 1988.

[3] X. Zhu and J. M. Kahn, "Free-space optical communication through atmospheric turbulence channels," *IEEE Trans. Commun.*, vol. 50, pp. 1293-1300, Aug. 2002.

[4] D. J. T. Heatley, D. R. Wisely, I. Neild, and P. Cochrane, "Optical wireless: the story so far," *IEEE Commun. Mag.*, pp. 72-74, 79-82, Dec. 1998.

[5] P. Smyth *et al.*, "Optical wireless–a prognosis," *Proc. SPIE*, 1995.

[6] C. E. Shannon, "Coding theorems for a discrete source with a fidelity criterion," *IRE Nat. Conv. Record*, part 4, pp. 142-163, 1959.

[7] A. J. Goldsmith and P. P. Varaiya, "Capacity of fading channels with channel side information," *IEEE Trans. Inform. Theory*, vol. 43, pp. 1986-1992, Nov. 1997.

[8] L. R. Bahl, J. Cocke, F. Jelinek, and J. Raviv, "Optimal decoding of linear codes for minimizing symbol error rate," *IEEE Trans. Inform. Theory*, vol. 20, pp. 284-287, Mar. 1974.

[9] J. Li, and M. Uysal, "Achievable information rate for outdoor free space optical communication with intensity modulation and direct detection," *Proc. GLOBECOM*, to appear, San Francisco, Nov. 2003.

[10] G. C. Clark, Jr. and J. B. Cain, *Error-correction coding for digital communications*, Plenum Press, NY, 1981.

[11] J. Li, *Low-Complexity, Capacity-Approaching Coding Schemes: Design, Analysis and Performance*, Ph.D. Dissertation, Texas A&M University, 2002; available online: http:// www.eecs.lehigh.edu/ ∼jingli/ publications.html.